Journal of Oil Palm Research
DOI: https://doi.org/10.21894/jopr.2026.0050

PRELIMINARY MORPHOMOLECULAR CHARACTERISATION OF A CRYPTIC WEEVIL ASSOCIATED WITH YOUNG OIL PALMS IN MALAYSIA

NUR AIN FARHAH ROS SAIDON KHUDRI[1]*; SITI NURULHIDAYAH AHMAD[1]; MOHD SHAWAL THAKIB MAIDIN[1]; NURHAFIZHOH ZAINUDDIN[1]; SHAMSILAWANI AHAMED BAKERI[1]; NOORHAZWANI KAMARUDIN[1] and MOHAMED MAZMIRA MOHD MASRI[1]

ABSTRACT

A cryptic weevil associated with damaged young oil palms was detected in Tangkak, Johor, Malaysia. The specimen was initially suspected to be the red palm weevil, Rhynchophorus ferrugineus*, but exhibited notable differences in body size and elytral markings. Morphometric analysis revealed morphological differences, prompting molecular identification using cytochrome c oxidase subunit I (*COI*) and 16S ribosomal RNA (*16S rRNA*) gene markers.* COI *sequence analysis showed 84.94%–85.17% identity with* Sphenophorus compressirostris*, while* 16S rRN*A analysis showed 93.36% identity with* Sparganobasis subcruciata *and 91.94% with* Sphenophorus *sp. These results suggest a closer phylogenetic affinity to* Sphenophorus- *or* Sparganobasis-*like taxa than to* Rhynchophorus*, although they should be interpreted as preliminary indications rather than definitive taxonomic placement. This study provides preliminary evidence of an unusual weevil lineage associated with Malaysian oil palm systems. The findings highlight the limitations of morphology-based identification alone and emphasise the value of integrating molecular diagnostics in pest surveillance. Given that related taxa include basal-boring species capable of damaging internal palm tissues, misidentification may result in inappropriate control strategies and overlooked infestations. Overall, this preliminary work underscores the importance of combining morphological and molecular approaches to improve diagnostic accuracy and support timely, evidence-based pest management in the oil palm industry.*

Keywords: *16S rRNA*, cytochrome c oxidase subunit I, *Elaeis guineensis*, morphology.

Received: 1 September 2025**; Accepted:** 26 August 2026**; Published online:** 3 November 2026.

ARTICLE IN PRESS

INTRODUCTION

Oil palm (*Elaeis guineensis* Jacq.) is a globally important oil crop and a key contributor to Malaysia's economy, covering approximately 5.65 million hectares and generating RM94.65 billion in export earnings from palm oil and its products in 2023 (Krishnan & Pimid, 2024; Parveez et al., 2024). Managing insect pests in oil palm is shifting away from highly visible canopy defoliators such as bagworms toward cryptic, internal-feeding species that easily escape standard visual inspection. Among these, palm-associated weevils within the Curculionidae family present a severe and escalating biosecurity threat. Pests such as the invasive red palm weevil (*Rhynchophorus ferrugineus*), *R. bilineatus*, *Sparganobasis subcruciata* and *Rhabdoscelus obscurus* are notorious for boring habits that devastate palm vascular tissues from the inside out (Khudri et al., 2021; Parveez et al., 2024; Priwiratama et al., 2019). These weevils frequently go unnoticed until the palm suffers irreversible structural damage because their destructive larval phases remain concealed within the host.

[1] Malaysian Palm Oil Board,
6, Persiaran Institusi, Bandar Baru Bangi,
43000 Kajang, Selangor, Malaysia.

* *Corresponding author e-mail: ainfarhah@mpob.gov.my*

This cryptic lifestyle makes early detection particularly important, yet the taxonomy of these weevils is notoriously difficult to navigate. Overlapping morphological characters, high phenotypic plasticity and unrecognised species complexes mean that identifying a specimen based purely on external features is highly unreliable. Misidentification may compromise surveillance programmes and result in inappropriate management decisions. Integrative taxonomy, combining morphological examination with DNA barcoding, has therefore become an important approach for resolving cryptic diversity and improving species delimitation in weevils and other insects. The cytochrome c oxidase subunit I (*COI*) gene is widely recognised as the standard DNA barcode for animal species identification, while the 16S ribosomal RNA (*16S rRNA*) gene provides complementary phylogenetic information for evaluating taxonomic affinity.

In 2018, an oil palm smallholding in Tangkak, Johor, Malaysia, intercropped with sweet potato, experienced unexpected mortality of recently replanted palms. Field inspection revealed adult weevils resembling the red palm weevil, *R. ferrugineus*, but differing noticeably in body size and external colour pattern, raising uncertainty regarding their taxonomic identity. Given the importance of accurate species recognition for pest surveillance, this study aimed to document the occurrence of these atypical weevils and to provide preliminary morphometric and molecular evidence using *COI* and *16S rRNA* gene markers to assess their taxonomic identity. As a short communication, this study provides an initial report intended to alert the oil palm industry and research community to the possible occurrence of a previously unrecognised palm-associated weevil in Malaysia while acknowledging that definitive taxonomic placement will require additional specimens, comprehensive morphological examination and expanded phylogenetic analyses.

MATERIALS AND METHODS

Sample Collection and Damage Assessment of Oil Palm Seedlings

All weevils (n = 3) were manually collected from the oil palm smallholding in Tangkak, Johor (2° 16′ 15.96″ N, 102° 32′ 31.20″ E) directly from infested young palms on 8 January 2018. The palms were also assessed during the visit to determine the extent of the damage due to the infestation. During transportation to the laboratory, the adult weevils were provided with chipped sugarcane as a temporary food source to maintain their viability.

Morphological Identification

A stereozoom microscope (Olympus SZ61, Olympus, Japan), integrated with ToupView software (version 4.1, ToupTek, China) and a high-resolution digital camera (Olympus, Japan), was used for detailed morphological examination of the collected weevils. This setup enabled precise measurement and high-quality imaging of key anatomical structures, including the head, antennae, rostrum, pronotum, thorax, scutellum, abdomen, elytra, femur, tibia and tarsus. The software's calibrated scale function enables accurate size assessment, aiding in species differentiation. The morphological assessment was conducted following the standardised procedure outlined in previous studies (Aziz et al., 2024; Ul Haq et al., 2018; Vaurie, 1951; Wattanapongsiri, 1966).

To further validate the morphological identification, the specimens were cross-referenced with authenticated insect collections housed at the Department of Agriculture of Malaysia. This comparison was conducted to assess morphological similarity and potential taxonomic affinity against diagnostic traits with previously documented specimens in the entomological archives.

Molecular Identification

DNA extraction. Molecular analyses were conducted to assess the taxonomic affinity of the three collected weevil specimens. Initially, 0.3 g of leg tissue was homogenised with liquid nitrogen to facilitate cell lysis. Extraction was performed using the InnuPREP DNA Mini Kit (Analytik Jena, Germany), following the manufacturer's protocol with minor modifications to optimise DNA yield. The extracted DNA was resuspended in 50 µL of elution buffer and stored at -20°C for preservation.

The assessment of DNA quality and concentration was performed using the NanoPhotometer spectrophotometer (Implen P300, USA) and Qubit™ dsDNA BR Assay Kit on a Qubit 2.0 Fluorometer (Life Technologies, USA), respectively.

Polymerase Chain Reaction (PCR) Amplification. The extracted genomic DNA was amplified using universal *COI* primers for molecular identification, LCO1490 (5′-GGTCAACAAATCATAAAGATAT TGG-3′) and HCO2198 (5′-TAAACTTCAGGGT GACCAAAAAATCA-3′) (Folmer et al., 1994), along with *16S rRNA* primers, 16S-5′ (CGCCTG TTTATCAAAAACAT) and 16S-3′ (CCGGTCTG AACTCAGATCACGT) (Ivanova et al., 2007). PCR amplifications for both *COI* and *16S rRNA* genes were performed in a 25 µL reaction mixture containing 16.75 µL molecular-grade water, 2.5 µL of 10× PCR buffer, 2.5 µL of $MgCl_2$ (15 mM), 1.0 µL

ARTICLE IN PRESS

of dNTPs (40 mM), 1.0 µL of each primer (1 mM), 0.25 µL of *Taq* DNA polymerase and 1.0 µL of DNA template. The PCR thermal cycling conditions included an initial denaturation at 95°C for 10.0 min, followed by 35 cycles of denaturation at 94°C for 1.0 min, annealing at 48°C for 1.0 min, and extension at 72°C for 1.5 min, with a final extension step at 72°C for 7.0 min. Amplified PCR products were visualised on a 1% agarose gel. The unpurified PCR products were subsequently submitted for sequencing (Apical Scientific, Malaysia).

Statistical Analysis

All morphometric measurements were recorded in millimetres (mm) and presented as mean ± standard error (SE). Descriptive statistical analyses, including the calculation of mean values, standard errors and data variability, were performed using Microsoft Excel (Microsoft Corporation, USA).

Mitochondrial *COI* and *16S rRNA* gene sequences obtained from this study and relevant reference taxa were first inspected and manually edited in BioEdit Version 7.7.1 (Hall, 1999) to correct sequencing ambiguities and remove poorly aligned end regions. All sequences were aligned using appropriate multiple sequence alignment methods, ensuring positional homology. The final trimmed alignment included a 669 bp fragment for *COI* and a 236 bp fragment for *16S rRNA*. The *16S rRNA* sequences were trimmed substantially from the initial 500–600 bp amplicons to remove low-quality terminal regions and sequencing artefacts, ensuring a high-confidence alignment of 236 bp for phylogenetic analysis.

Substitution model selection and maximum-likelihood tree estimation. Phylogenetic trees were constructed using the maximum-likelihood (ML) approach implemented in IQ-TREE multicore v2.0.7 for Linux 64-bit (Nguyen et al., 2015). The best-fit nucleotide substitution model for each dataset was automatically determined using the integrated ModelFinder algorithm (Kalyaanamoorthy et al., 2017) under the Bayesian Information Criterion (BIC). To assess node support, 1,000 ultrafast bootstrap replicates (Hoang et al., 2018) and SH-aLRT tests with 1,000 replicates were performed in the same run. The trees were visualised and annotated using FigTree v1.4.4 (Rambaut, 2018).

RESULTS AND DISCUSSION

Damage Assessment of Oil Palm Seedlings

Field assessments at an oil palm smallholding in Tangkak, Johor, revealed that 53 out of 378 surveyed young oil palms exhibited clear symptoms of internal damage. Externally, these affected palms appeared completely intact. Destructive sampling showed severe internal tissue rot concentrated within their basal regions. Splitting the stems open exposed active larval feeding galleries packed with accumulated frass (*Figure 1*).

A total of three adult weevils (n = 3) were recovered from these affected palms. The visible damage sequence begins with overall wilting, drying fronds and a chlorotic emerging spear leaf. In late-stage infestations, this progresses to complete desiccation and palm mortality. Because this baseline dataset relies on a small initial cohort, these findings must be treated strictly as preliminary field observations that require broader geographic validation.



Figure 1. Visual symptoms of oil palm seedlings infested by cryptic weevil. (a) Wilted and desiccated young oil palm seedling with emerging chlorotic spear leaf, indicating internal tissue damage, (b) longitudinal section of a damaged frond showing the presence of weevil larva (red arrow) within the feeding gallery, (c) cross-sectional view of the rotten spear base showing extensive internal damage and frass accumulation (red arrow), typical of larval feeding activity and (d) severely dried and wilted seedling indicating late stage of infestation.

Morphological and Morphometric Interpretation of the Cryptic Weevil

The three collected adult weevils exhibited general morphological characteristics consistent

ARTICLE IN PRESS

with the family Curculionidae, including an elongated oval body, a moderately curved rostrum and clubbed antennae (*Figure 2*). Body colouration ranged from dark brown to black, with relatively small yellowish-orange markings on the elytra. These markings are distinctly smaller and less pronounced than the bright, broad reddish-orange configurations characteristic of *R. ferrugineus* (European and Mediterranean Plant Protection Organization [OEPP/EPPO], 2007). The head was relatively small compared to the thorax, with well-defined compound eyes positioned laterally. The rostrum was short relative to body size, differing from typical *Rhynchophorus* sp. morphology.



Figure 2. Morphological appearance of adult weevil collected from the infested young oil palms in Tangkak, Johor.

The pronotum displayed distinct sculpturing, with a slightly wider anterior margin tapering towards the posterior. The elytra were fused, covered the entire abdomen and displayed fine longitudinal striations. The legs were well-developed, with a robust femur and tibia, while the tarsal claws were small but curved, adapted for gripping plant surfaces.

The three weevil specimens were then subjected to morphometric analysis. The mean body measurements (± SE) of key anatomical structures are presented in *Table 1*.

The weevils exhibited a compact body structure, with total body length ranging from approximately 12.00 to 15.00 mm (12.61 ± 0.76) compared to the much larger 30.00 to 31.20 mm range seen in *R. ferrugineus* (Ul Haq et al., 2018). The rostrum length ranged from 1.11 to 1.42 mm (1.26 ± 0.16 mm), representing approximately 10% of the total body length. The pronotum was slightly longer than wide (1.48 ± 0.05 vs. 1.11 ± 0.02 mm, respectively), with a distinct sculptured surface.

The elytral length averaged 2.00 ± 0.04 mm, covering the entire dorsal region and displaying a dark brown to black colouration with small orange markings. The femur and tibia lengths were measured at 0.87 ± 0.06 and 0.50 ± 0.04 mm, respectively, while the tarsus length of 0.50 ± 0.06 mm suggested adaptations for strong grip and movement within palm tissues.

In brief, morphological observations and morphometric measurements indicate that the collected specimens differ from *R. ferrugineus* in overall size, body proportions and elytral patterning (*Table 2*) (OEPP/EPPO, 2007). However, given the limited sample size (n = 3) and the absence of detailed examination of key diagnostic characters (e.g., genitalia, antennal segmentation, tarsal formula), these differences should not be considered definitive evidence of distinct taxonomic status. Rather, the observed variation is best interpreted as indicative of potential taxonomic divergence that warrants further investigation.

TABLE 1. MORPHOMETRIC MEASUREMENTS OF THE CRYPTIC WEEVIL COLLECTED FROM AN OIL PALM SMALLHOLDING IN TANGKAK, JOHOR

Parameter	Sample Number	Measurement (mm)	Mean ± SE (mm)
Head length	1	1.28	1.44 ± 0.18
	2	1.63	
	3	1.40	
Head width	1	0.38	0.36 ± 0.02
	2	0.34	
	3	0.36	
Antennal length	1	0.94	1.02 ± 0.09
	2	1.00	
	3	1.12	
Rostrum length	1	1.11	1.26 ± 0.16
	2	1.42	
	3	1.24	
Pronotum length	1	1.47	1.48 ± 0.05
	2	1.44	
	3	1.54	
Pronotum width	1	1.12	1.11 ± 0.02
	2	1.09	
	3	1.13	
Thorax length	1	2.20	2.23 ± 0.12
	2	2.13	
	3	2.36	
Scutellum length	1	0.29	0.25 ± 0.03
	2	0.23	
	3	0.24	
Abdomen length	1	7.37	7.68 ± 0.3
	2	8.01	
	3	7.66	
Elytral length	1	2.00	2.00 ± 0.04
	2	1.96	
	3	2.04	
Femur	1	0.82	0.87 ± 0.06
	2	0.93	
	3	0.87	
Tibia	1	0.53	0.50 ± 0.04
	2	0.46	
	3	0.52	
Tarsus	1	0.57	0.50 ± 0.06
	2	0.47	
	3	0.47	

ARTICLE IN PRESS

TABLE 2. COMPARATIVE MORPHOMETRIC MEASUREMENTS OF THE CRYPTIC WEEVIL WITH *Rhynchophorus ferrugineus*

Morphological trait	Cryptic weevil (Mean ± SE) (mm)	References	*Rhynchophorus ferrugineus* (Typical range) (mm)	Reference
Total body length	12.61 ± 0.76	This study	30–31.2	Ul Haq et al. (2018)
Head length	1.44 ± 0.18	This study	7.7–8.7	Ul Haq et al. (2018)
Rostrum length	1.26 ± 0.16	This study	5.0–8.0	Ul Haq et al. (2018)
Abdomen length	7.68 ± 0.3	This study	12.0–26.0	Ul Haq et al. (2018)
Pronotum width	1.11 ± 0.02	This study	8.55–8.70	Ul Haq et al. (2018)

Molecular Interpretation and Taxonomic Placement of Cryptic Weevil

Mitochondrial *COI* and *16S rRNA* gene sequences were generated and used to evaluate the taxonomic placement of the collected specimens to overcome the limitations of morphology-based identification, particularly those associated with convergent evolution and colour polymorphism (*Figure 3* and *4*).

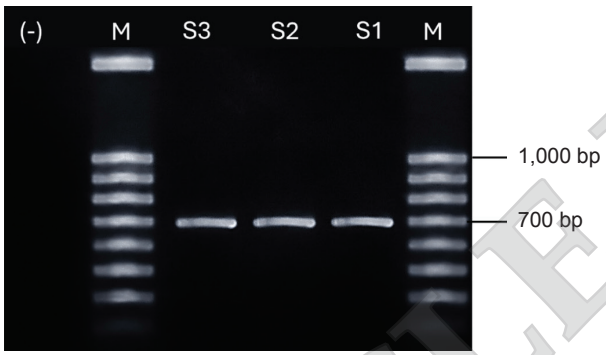


*Figure 3. Agarose gel electrophoresis image of polymerase chain reaction (PCR) amplification products targeting the cytochrome c oxidase subunit I (*COI*) gene in cryptic weevil samples. A single, distinct band of approximately 700 bp is observed in samples S1, S2 and S3, confirming successful amplification. Lane M - 1 kb plus DNA ladder; Lanes S1–S3 - individual weevil samples; Lane (–) - negative control (no template DNA).*

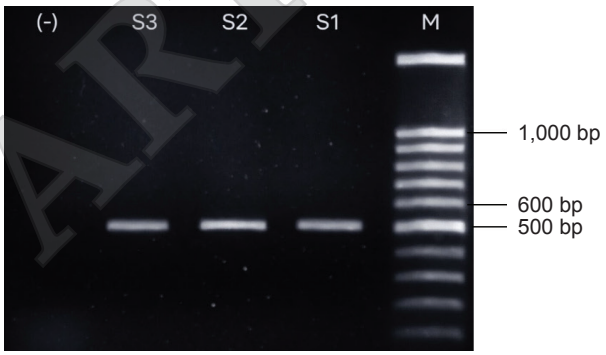


Figure 4. Agarose gel electrophoresis image of polymerase chain reaction (PCR) amplification products targeting the 16S rRNA *gene in cryptic weevil samples. A single, distinct band of approximately 500–600 bp is observed in samples S1, S2 and S3, confirming successful amplification. Lane M - 1 kb plus DNA ladder; Lanes S1–S3 - individual weevil samples; Lane (–) - negative control (no template DNA).*

Gel electrophoresis verified clean, successful PCR amplification, showing single bands at approximately 700 bp for *COI* and between 500–600 bp for *16S rRNA* across all three samples.

Basic local alignment search tool (BLAST) analysis of the *COI* sequences demonstrated the highest similarity to *Sphenophorus compressirostris*, though with a modest percentage identity of 84.94%–85.17% (*Table 3*). Other closely related matches included species from the subfamily *Brachycerinae*, such as *Brachyderes incanus* and *Brachycerinae* sp., with sequence identities between 84.51% and 84.75%, respectively. Notably, *COI* BLAST results did not recover *Rhynchophorus* spp. among the closest matches.

These findings from *COI* sequences suggest that the collected weevils are more closely related to *Sphenophorus* or a taxonomically allied genus within *Brachycerinae* rather than *R. ferrugineus*. The relatively moderate sequence similarity (below 90%) suggests the possibility of cryptic diversity, population variation or even an undescribed taxon within the group.

TABLE 3. NUCLEOTIDE BASIC LOCAL ALIGNMENT SEARCH TOOL (BLAST) OF Cytochrome c oxidase subunit I (*COI*) GENE

Description	Percentage identity (%)	Accession	E-value
Sphenophorus compressirostris	84.94	HQ984445.1	0.0
Sphenophorus compressirostris	85.17	HM433171.1	8e-180
Brachycerinae sp.	84.75	MW201360.1	1e-177
Brachyderes incanus	84.51	KJ965002.1	2e-176
Ubychia sp.	83.66	PP889716.1	6e-176

The COI maximum-likelihood tree (*Figure 5*) shows that the cryptic weevil sequence occupies a distinct lineage basal to the clade containing representative sequences of the subfamily *Brachycerinae*. While BLAST results indicated sequence similarity to *Sphenophorus*-like taxa, the phylogenetic placement highlights a distinct

ARTICLE IN PRESS

evolutionary separation from both the *Brachycerinae* clade and the well-supported *R. ferrugineus* lineage. Notably, *HQ984445.1* (*S. compressirostris*), *KJ965002.1* (*Brachyderes incanus*), *PP889716.1* (*Ubychia* sp.) and *MW201360.1* (*Brachycerinae* sp.) formed a well-supported clade with bootstrap values >70 at key internal nodes (e.g., 76% between *PP889716.1* and its sister taxa). In contrast, *HM433171.1* (*S. compressirostris*) occupied a more basal position outside this clade, together with the outgroup taxon *AY131104.1*. The weevil specimen occupies a basal position relative to the clade containing *KU916538.1* (*R. ferrugineus*), for which bootstrap support was 72%. Importantly, the node separating the cryptic weevil from the *R. ferrugineus* lineage received robust support (100%) (*Figure 5*), corroborating BLAST results that indicated greater genetic affinity with *Sphenophorus*-like taxa (84.94%–85.17% sequence identity; *Table 3*). Because *COI* is widely used as a species-level marker in DNA barcoding (Hebert et al., 2003), its phylogenetic placement lends weight to the assertion that the collected specimens likely represent a taxon within *Brachycerinae* distinct from widely characterised pests like *R. ferrugineus*.

BLAST analysis of the amplified *16S rRNA* gene sequence also revealed significant alignments with several Curculionidae species (*Table 4*). The highest identity match (93.36%) was observed with *S. subcruciata* isolate COL1241 (GenBank accession: *KF016274.1*), covering 75% of the query sequence with an E-value of 1e–79, suggesting a close phylogenetic relationship. The second-highest alignment was with *Sphenophorus* sp. BYU-CO246 (accession: *NC_018351.1*), showing a 91.94% identity across 74% of the query, with an E-value of 5e–74, while the well-documented oil palm pest *R. ferrugineus* (accession: KT428893.1) ranked fifth, with 89.18% identity and 82% query coverage (E-value: 2e–72).

These results indicate that the sequenced weevil shares greater genetic affinity with *Sparganobasis* and *Sphenophorus* genera than with *Rhynchophorus*, challenging prior assumptions based solely on morphological identification. Previous studies have highlighted the limitations of morphological approaches in distinguishing closely related weevil species, emphasising the necessity of molecular techniques for accurate identification (Hallett et al., 2004; Rugman-Jones et al., 2013). The relatively high identity scores with both *S. subcruciata* and *Sphenophorus* spp. underscore the need for further phylogenetic resolution and taxonomic clarification, as these genera include basal borers with cryptic life stages.

TABLE 4. NUCLEOTIDE BASIC LOCAL ALIGNMENT SEARCH TOOL (BLAST) OF *16S rRNA* GENE

Description	Percentage identity (%)	Accession	E-value
Sparganobasis subcruciata	93.36	KF016274.1	1e-79
Sphenophorus sp.	91.94	NC_018351.1	5e-74
Rhynchophorus ferrugineus	89.18	KT428893.1	2e-72
Phacecorynes variegatus	90.09	AJ495599.1	8e-72
Cryptoderma sp.	89.82	LN888353.1	8e-72

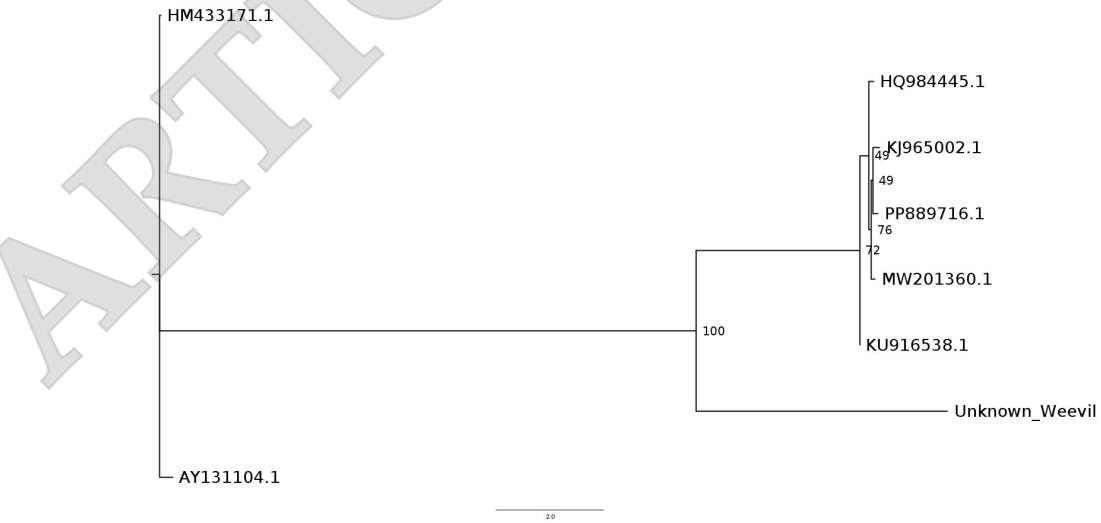


*Figure 5. Maximum-likelihood phylogenetic tree inferred from mitochondrial cytochrome c oxidase subunit I (*COI*) gene sequences showing the relationship between the cryptic weevil specimen and selected Curculionidae taxa. The tree was constructed using IQ-TREE v2.0.7 under the best-fit substitution model determined by ModelFinder, with 1,000 ultrafast bootstrap replicates. Bootstrap support values (%) greater than 50 are indicated at the nodes.*

ARTICLE IN PRESS

The *16S rRNA* gene phylogeny (*Figure 6*) reinforces the molecular distinction of the cryptic weevil from *Rhynchophorus*. The cryptic weevil clusters specifically with *S. subcruciata* (KF016274.1), which is consistent with the highest BLAST identity value of 93.36%. Conversely, *Sphenophorus* sp. (NC_018351.1) is positioned on a separate, well-supported branch alongside *R. ferrugineus*. While the bootstrap support for deeper nodes was moderate, the grouping of the cryptic weevil with these taxa was consistently supported across replicates, indicating a shared evolutionary history distinct from more distantly related taxa such as KT428893.1 (*R. ferrugineus*) and other Curculionidae references. Although some internal branches exhibited lower bootstrap values (<50), the overall tree topology was congruent with the expectation based on sequence similarity and taxonomic affiliation.

Accurate species identification is fundamental in entomological research, particularly in the context of pest management and ecological assessment. In this study, molecular analyses indicate that the collected weevil specimens show closer sequence similarity to *S. subcruciata* and *Sphenophorus* spp. than to the well-documented pest *R. ferrugineus*. This observation is noteworthy, as initial identification based on external morphology alone suggested affinity with *R. ferrugineus*, highlighting the limitations of morphology-based diagnostics. Nevertheless, the BLAST-based results presented here should be interpreted as preliminary phylogenetic indications rather than definitive taxonomic assignments. Further analyses, including expanded sampling and phylogenetic reconstruction, are required to confirm the taxonomic placement of these specimens. The *COI* gene, commonly employed for species-level identification, revealed significant alignment with *S. compressirostris* and other *Brachycerinae* members such as *B. incanus* and *Bordoniola* sp. (Hebert et al., 2003). Notably, none of the top BLAST hits suggested a strong match with *Rhynchophorus* spp., indicating that the initial morphological classification was likely misleading. This finding underscores the limitations of morphological identification, particularly in cases where convergent evolution or intraspecific variation can obscure diagnostic traits.

The *COI* similarity values (~85%) fall below commonly applied thresholds for confident genus- or species-level assignment, and while our maximum-likelihood phylogenetic reconstructions support a divergence from *Rhynchophorus*, the low sequence identities mean our current inferences rely on sequence similarity and preliminary topological placement to assess broad taxonomic affinity, rather than confirming species-level identity. Therefore, we interpret these findings as preliminary phylogenetic indications of affinity with *Sphenophorus*- or *Sparganobasis*-like lineages rather than definitive taxonomic placement. Expanded sampling, detailed examination of additional diagnostic morphological characters (including genitalia) and robust phylogenetic analyses are required to resolve evolutionary relationships with confidence.

Sphenophorus spp., although typically associated with grasses and cereals (Ordaz-González et al., 2014), are increasingly being reported in non-traditional hosts, suggesting either a broader host range or adaptive shifts

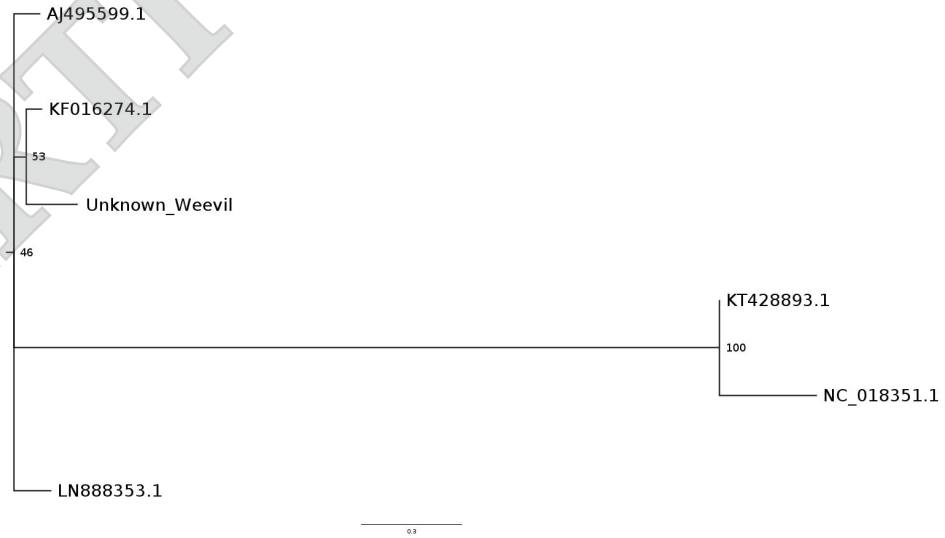


Figure 6. Maximum-likelihood phylogenetic tree inferred from mitochondrial 16S rRNA *gene sequences showing the relationship between the unknown weevil specimen (cryptic weevil) and selected Curculionidae taxa. The tree was constructed using IQ-TREE v2.0.7 under the best-fit substitution model determined by ModelFinder, with 1,000 ultrafast bootstrap replicates. Bootstrap support values (%) greater than 50 are indicated at the nodes.*

ARTICLE IN PRESS

under monoculture conditions (El-Maghraby et al., 2022). *Sphenophorus* spp., often misidentified or overlooked due to their morphological similarity to *Rhynchophorus* spp., have recently been implicated in the early mortality of young palms. These cryptic weevils cause significant internal damage by boring into the basal regions and feeding on vascular tissues, often without clear external symptoms, which delays detection and complicates management.

Likewise, the top BLAST hit, *S. subcruciata*, has been reported as a basal boring weevil in association with decaying tissues of oil palm in Papua New Guinea (Dewhurst & Pilotti, 2012; Priwiratama et al., 2019), but its pest status in Malaysia remains undocumented. The detection of *Sparganobasis* and *Sphenophorus* DNA over *R. ferrugineus* raises important questions regarding pest surveillance in oil palm systems. Given the similar cryptic appearance of these species, particularly in larval and pupal stages, misidentifications are not only likely but may already have impacted the efficacy of control programmes designed specifically for *R. ferrugineus*. This highlights a broader issue in pest diagnostics, where visual identification is insufficient to distinguish between closely related or convergently evolved species (Sheth & Thaker, 2017). Previous research has shown that the misidentification of red palm weevil populations has occurred even between *R. ferrugineus* and *R. vulneratus* until molecular phylogenetics clarified their taxonomy (Hallett et al., 2004; Rugman-Jones et al., 2013).

Given our limited sample size (n = 3), these ecological implications remain preliminary hypotheses. If *S. subcruciata* or *Sphenophorus* spp. are indeed present in oil palm plantations, further baseline monitoring is warranted to clarify their infestation dynamics, larval development habits and host preferences. This is a relevant consideration as both genera include species known for basal boring and internal tissue feeding. These traits can lead to concealed damage in young palms until irreversible wilt or mortality occurs. Furthermore, while speculative at this stage, a potential association with decaying or pathogen-infected tissue as observed with *Ganoderma* spp. in other weevil-host interactions opens the possibility of synergistic impacts that might worsen disease severity or pest establishment. Further work involving larger sample sizes, broader field surveys, life-history studies and host-association assessments will be needed to better understand the role of this taxon in oil palm ecosystems. Such investigations will help determine whether these specimens represent an isolated finding, a species that has previously gone unnoticed or a taxon with potential economic relevance to the oil palm industry.

CONCLUSION

This study documents the detection of a morphologically atypical curculionid associated with young oil palms in Johor, initially suspected to be *R. ferrugineus* but showing morphometric and molecular divergence from that species. Molecular results based on *COI* and *16S rRNA* gene markers suggest greater affinity with *Sphenophorus*- and *Sparganobasis*-like lineages than with *Rhynchophorus* spp., highlighting the limitations of morphology-based identification alone and the importance of incorporating molecular diagnostics into pest surveillance frameworks. However, given the limited sample size (n = 3), reliance on initial BLAST similarities and preliminary phylogenetic clustering, alongside the absence of comprehensive diagnostic morphological examination, these findings should be interpreted as provisional rather than definitive. Future studies incorporating broader sampling and integrative taxonomic approaches are required to resolve the identity and ecological significance of this weevil. This study highlights the value of combining DNA barcoding with morphometric analyses to improve diagnostic accuracy and strengthen early pest surveillance in oil palm ecosystems.

ACKNOWLEDGEMENT

The authors would like to express their gratitude to the Director-General of MPOB for granting permission to publish this article. The authors also extend their gratitude to the dedicated staff of the Entomology and Integrated Pest Management Unit of MPOB for their invaluable support in conducting this study. The authors also express their heartfelt appreciation to all individuals who contributed to this research, both directly and indirectly.

REFERENCES

Aziz, D., Ahad, I., Shah, Z. A., Khan, Z. H., Dar, E. A., Alie, B. A., Lone, A. H., Ganie, M. A., Alkeridis, L. A., Al-Shuraym, L. A., Sayed, S., & Shukry, M. (2024). Morphomolecular characterization of invasive fruit borer infesting apple. *Scientific Reports, 14*, 11972. https://doi.org/10.1038/s41598-024-61585-3

Dewhurst, C. F., & Pilotti, C. A. (2012). First record of the base-borer weevil, *Sparganobasis subcruciata* Marshall (Coleoptera: Curculionidae: Dryopthorinae), from oil palm (*Elaeis guineensis* Jacq.) in Papua New Guinea and its association with decaying stem tissue. *The Australian Entomologist, 39*(3), 197–207.

ARTICLE IN PRESS

El-Maghraby, W. T. Q. H., Kadada, H. M., & Elshaier, M. E. A. (2022). New record of the billbug genus *Sphenophorus* Schoenherr, 1838 (Coleoptera: Curculionidae: Dryophthorinae) from Egypt. *Egyptian Academic Journal of Biological Sciences, 15*(3), 9–14. https://doi.org/10.21608/eajbsa.2022.249408

European and Mediterranean Plant Protection Organization (OEPP/EPPO). (2007). EPPO standard PM 7/83 diagnostics: *Rhynchophorus ferrugineus* and *Rhynchophorus palmarum*. *EPPO Bulletin, 37*(3), 571–579. https://doi.org/10.1111/j.1365-2338.2007.01165.x

Folmer, O., Black, M., Hoeh, W., Lutz, R., & Vrijenhoek, R. (1994). DNA primers for amplification of mitochondrial *cytochrome c oxidase subunit I* from diverse metazoan invertebrates. *Molecular Marine Biology and Biotechnology, 3*(5), 294–299.

Hall, T. A. (1999). BioEdit: A user-friendly biological sequence alignment editor and analysis program for Windows 95/98/NT. *Nucleic Acids Symposium Series*, *41*, 95–98.

Hallett, R. H., Crespi, B. J., & Borden, J. H. (2004). Synonymy of *Rhynchophorus ferrugineus* (Olivier), 1790 and *R. vulneratus* (Panzer), 1798 (Coleoptera, Curculionidae, Rhynchophorinae). *Journal of Natural History, 38*(22), 2863–2882. https://doi.org/10.1080/00222930310001657874

Hebert, P. D. N., Cywinska, A., Ball, S. L., & deWaard, J. R. (2003). Biological identifications through DNA barcodes. *Proceedings of the Royal Society B: Biological Sciences, 270*(1512), 313–321. https://doi.org/10.1098/rspb.2002.2218

Hoang, D. T., Chernomor, O., von Haeseler, A., Minh, B. Q., & Vinh, L. S. (2018). UFBoot2: Improving the ultrafast bootstrap approximation. *Molecular Biology and Evolution*, *35*(2), 518–522. https://doi.org/10.1093/molbev/msx281

Ivanova, N. V., Zemlak, T. S., Hanner, R. H., & Hebert, P. D. N. (2007). Universal primer cocktails for fish DNA barcoding. *Molecular Ecology Notes 7*(4), 544–548. https://doi.org/10.1111/j.1471-8286.2007.01748.x

Kalyaanamoorthy, S., Minh, B. Q., Wong, T. K. F., von Haeseler, A., & Jermiin, L. S. (2017). ModelFinder: Fast model selection for accurate phylogenetic estimates. *Nature Methods*, *14*(6), 587–589. https://doi.org/10.1038/nmeth.4285

Khudri, N. A. F. R. S., Masri, M. M. M., Maidin, M. S. T., Kamarudin, N., Hussain, M. H., Abd Ghani, I., & Jalinas, J. (2021). Preliminary evaluation of acoustic sensors for early detection of red palm weevil, *Rhynchophorus ferrugineus* incidence on oil palm and coconut in Malaysia. *International Journal of Tropical Insect Science, 41*(4), 3287–3292. https://doi.org/10.1007/s42690-021-00499-3

Krishnan, K. T., & Pimid, M. (2024). Understanding the effects of climate change on *Elaidobius kamerunicus* (Coleoptera: Curculionidea), an important oil palm pollinator in Malaysia: Predicting future distribution for the year 2050 under different climate pathways. *Malaysian Applied Biology, 53* (6), 167–177. https://doi.org/10.55230/mabjournal.v53i6.11

Nguyen, L. T., Schmidt, H. A., von Haeseler, A., & Minh, B. Q. (2015). IQ-TREE: A fast and effective stochastic algorithm for estimating maximum-likelihood phylogenies. *Molecular Biology and Evolution*, *32*(1), 268–274. https://doi.org/10.1093/molbev/msu300

Ordaz-González, E. L., Equihua-Martínez, A., León-García, I., Jones, R. W., Aragón, A., Hernández Hernández, R., & Pineda S. V. (2014). Species of *Sphenophorus* (Coleoptera: Dryophthoridae) associated with golf courses in Mexico. *Florida Entomologist, 97*(2), 857–860. https://doi.org/10.1653/024.097.0280

Parveez, G. K. A., Leow, S. S., Kamil, N. N., Madihah, A. H., Ithnin, M., Ng, M. H., Yusof, Y. A., & Idris, Z. (2024). Oil palm economic performance in Malaysia and R&D progress in 2023. *Journal of Oil Palm Research, 36*(2), 171–186. https://doi.org/10.21894/jopr.2024.0037

Priwiratama, H., Prasetyo, A. E., Pradana, M. G., Rozziansha, T. A. P., Susanto, A., & de Chenon, D. R. (2019). Weevil stem borer and mesocarp-eating beetle: New threat to oil palm plantations in Indonesia. In *Proceedings of the PIPOC 2019 International Palm Oil Congress (Agriculture, Biotechnology & Sustainability)* (pp. 67–81).

Rambaut, A. (2018). *FigTree v1.4.4* [Computer software]. https://tree.bio.ed.ac.uk/software/figtree/

Rugman-Jones, P. F., Hoddle, C. D., Hoddle, M. S., & Stouthamer, R. (2013). The lesser of two weevils: Molecular-genetics of pest palm weevil populations confirm *Rhynchophorus vulneratus* (Panzer 1798) as a valid species distinct from *R. ferrugineus* (Olivier 1790), and reveal the global extent of both. *PLoS ONE, 8*(10), e78379. https://doi.org/10.1371/journal.pone.0078379

ARTICLE IN PRESS

Sheth, B. P., & Thaker, V. S. (2017). DNA barcoding and traditional taxonomy: An integrated approach for biodiversity conservation. *Genome, 60*(7), 618–628. https://doi.org/10.1139/gen-2015-0167

Ul Haq, I., Shams, S., Khan, S., Khan, A., & Hameed, A. (2018). A novel report on morphological study of red palm weevil (*Rhynchophorus ferrugineus*) from district Bannu KPK, Pakistan. *Cogent Food & Agriculture, 4*(1), 1425117. https://doi.org/10.1080/23311932.2018.1425117

Vaurie, P. (1951). Revision of the genus *Calendra* (formerly *Sphenophorus*) in the United States and Mexico (Coleoptera, Curculionidae). *Bulletin of the American Museum of Natural History, 98*, 29–186.

Wattanapongsiri, A. (1966). *A revision of the genera Rhynchophorus and Dynamis (Coleoptera: Curculionidae)* [Doctoral dissertation, Oregon State University].

ARTICLE IN PRESS